www.editada.org

International Journal of Combinatorial Optimization Problems and Informatics, 18(1), 2027, 401-417. ISSN: 2007-1558.
https://doi.org/10.61467/2007.1558.2027.v18i1.1517

Nested Sliding Surface in Robust Neuro Fuzzy Control for a Servomechanism System Regulation

Omar Samperio Vázquez[1], Jesús Patricio Ordaz Oliver [1]✉, and Julio Cesar Ramos-Fernandez[2].
[1] Universidad Autónoma del Estado de Hidalgo, Pachuca de Soto, Hidalgo, 42184, México
[2] Universidad Politécnica de Pachuca, Zempoala, Hidalgo, México
omarsamvaz@uaeh.edu.mx, jesus_ordaz@uaeh.edu.mx, jramos@upp.edu.mx.
✉Corresponding author: jesus_ordaz@uaeh.edu.mx

Abstract. This paper describes the design of a robust neuro-fuzzy control system for regulating a servomechanism, which is based on the development of a nested sliding-mode approach to effectively regulate the system and reduce the chattering effect. The approach involves developing a nested sliding mode control with gain adjustment using adaptive Neuro-Fuzzy Inference. Furthermore, the servomechanism is driven by the voltage applied to a DC motor, and the controlled outputs are the angular position and velocity of the shaft. One key feature of this advanced intelligent control system is its capability to efficiently regulate the position and speed of the servomechanism in an exponential sense, even in the presence of dynamic uncertainties and external disturbances. To this end, in the first step, a conditional nested sliding mode control was developed to reduce the magnitude of the chattering effect. However, the magnitude of this conditional controller produces chattering effects on the actuator. To reduce this issue, an Adaptive Neuro-Fuzzy Inference System suggests adjusting the control gains of the sliding modes. So, the proposed control scheme helps reduce the magnitude of the chattering effect in the control signal. To validate the proposed control strategy's effectiveness, a comparative study based on error criteria is presented, highlighting its potential on the control process.

Keywords: Nested, Neuro Fuzzy, Servomechanism.

Article information
Received: Jul 10, 2026
Accepted: Aug 10, 2026

1 Introduction

Mechanisms driven by DC motors are widely recognized as one of the most common laboratory prototypes used in control system education. This is because they are crucial elements for designing and controlling various applications in industrial processes, including servomechanisms, pendulum systems, robot manipulators, peristaltic pumps, among others. The above is due to its versatility in coupling with position and speed sensors, low cost, and robust implementation of control strategies. In the control theory study, the DC motor can be analyzed as either a SISO or SIMO system, depending on the operational requirements. When a DC motor is coupled to mechanical and electronic components to function as a servomechanism, the control of the servomechanism can be analyzed using either electric current or torque. The servomechanism output can be the position, velocity, or both, depending on the transducers that measure the system output. Nowadays, modern microcontrollers have high data processing capacity that enables the implementation of advanced control strategies in servomechanisms. For this reason, advanced control strategies such as sliding modes, neural networks, fuzzy logic, optimal control with delays, and those based on LMIs, output controllers based on observers, among others, can be efficiently implemented in control loops using small- and medium-scale microcontrollers (Cheng et al., 2024; Hu et al., 2024; Wang et al., 2024). In sliding mode control (SMC) of a servomechanism with an input voltage, the chattering effect negatively impacts the system performance (Shtessel et al., 2014; Utkin et al., 2020; Azar & Zhu, 2015). The SMC range includes various algorithms that can be categorized into five different generations. The first generation is the classical SMC. The next generation focuses on second-order SMC. The third generation introduces SMC based on the Super-Twisting Algorithms. The fourth generation of SMC deals with Arbitrary Order SMC (in this one, the nested SMC concept was introduced). Continuous arbitrary order SMC are considered as the Fifth Generation (Yu & Efe., 2015). However, SMC has several distinctive features compared to other robust control algorithms, one of which is its insensitivity to disturbances, a characteristic shared by most SMCs. Another important feature is the convergence of trajectories within a finite time achieved by employing terminal sliding mode (Cruz-Ortiz et al., 2022). However, the main issue in SMC is the chattering effect that occurs on the control signal. This effect can significantly reduce the actuators' lifespan or cause them to fail completely or degrade prematurely (Utkin & Lee., 2006). To reduce the magnitude of chattering effects, several algorithms have been suggested in the literature, however, completely mitigating it remains an open challenge. Using a first-order filter approximation instead of the sign function is a method to decrease the magnitude of chattering effects (Wang & Adeli., 2012). Nonetheless, this approach significantly diminishes the robustness of an SMC system. Another option is to use asymptotic sliding modes, but the effectiveness of this control may be compromised by the nature of the disturbances. On the other hand, using fuzzy algorithms can help reduce the magnitude of chattering, but it may lead to issues in the stability analysis of the closed-loop system (Lin et al., 2022; Hamzah et al., 2024; Yonezawa et al., 2025).

Fuzzy theory integrated into a Sliding Mode Control (SMCFz) offers several important features. One of the main advantages of this hybrid control system is the decrease in chattering (Wang & Adeli., 2012; Wong et al., 2001; Prieto et al.,2017; Feng et al., 2022). To effectively reduce the chattering effect in the FSMC, a human expert must provide reasoning to the fuzzy inference system. For instance, in (Ertugrul & Kynay., 2000), the SMC parameters are adjusted using adaptation algorithms based on fuzzy logic. In (Wang & Fei., 2022), a controller is introduced that combines terminal sliding-mode control with a recurrent Chebyshev fuzzy neural network. This controller utilizes a self-evolving mechanism to adaptively update its dynamic structure by generating and adjusting fuzzy logic rules. In (Li & Zhai., 2024), a fuzzy logic system has been integrated into the adaptive super-twisting sliding mode controller to estimate and compensate for system uncertainties. Therefore, applying the FSMC to a specific system requires the expertise of a user. Moreover, developing a fuzzy inference system using expert knowledge can result in a diverse set of fuzzy rules, a wide range of membership functions, and other key characteristics of the system. The issue mentioned can pose a challenge when implementing fuzzy controllers in a real-time control system. To reduce computational costs during implementation, algorithms such as Neuro-fuzzy systems have been developed (Li et al., 2020; Shaihi et al., 2023; Aydin & Yakut., 2023). The Adaptive Neuro-Fuzzy Inference System (ANFIS) is an algorithm that combines artificial neural networks and fuzzy logic to create a model capable of identifying a system based on its inputs and outputs (Yang et al., 2021; Asar et al., 2019; Yareshe et al., 2025).

In this paper, a nested sliding surface approach based on neuro-fuzzy control (SMCFz), a method is presented for tuning controller parameters, which improve the position and velocity control of the servomechanism using a hybrid control law. Additionally, the control action should be designed in a way that does not cause undue stress on the actuator. To achieve this, a robust control scheme based on asymptotic SMC was initially designed to regulate the position and velocity of the servomechanism. The system being discussed is of third order and is related to servo position, velocity, and electrical current. Due to the relative degree of the servo system, the dynamics of a single sliding surface σ related to position and velocity cannot achieve regulation. This means that a high-order sliding mode controller is a key point for regulating the servo system. In this case, to achieve control action that ensures sliding motion control, a Sliding Mode Controller is used instead of a high-order sliding mode controller. The second sliding surface takes into account the solution of the previous one. Additionally, to reduce the chattering effect caused by this control strategy, the gains of the nested SMC control are adjusted using an Adaptive Neuro-Fuzzy approach. This design is commonly referred to in the literature as nested sliding modes (Yu & Efe., 2015). Furthermore, to reduce the chattering effect caused by this control strategy, the control gains of the nested SMC are adjusted using an Adaptive Neuro-Fuzzy Inference System.

The gain adjustment was designed by initially generating it through the position errors of the servomotor. Now, with experimental measurements of the nested SMC, using that gain adjustment, the values of minimum error were sought in order to use the if conditional, that is, if $e < \epsilon$, then reduce the parameters λ_1, λ_2 which are decay gain (5) and (6) and ρ is a gain that mitigates the effects of uncertain dynamics and external disturbances (14). This technique will be referred to as SMCif.

Although the magnitude of the chattering effect was reduced, its intensity could still potentially harm the actuator. Consequently, a gain adjustment was developed using the acquired knowledge and applied to fuzzy logic. The issue identified was the high computational cost, rendering its implementation impractical. Finally, by employing ANFIS-based algorithms, a robust control system was successfully developed. Nevertheless, a chattering effect occurs on the control signal, potentially resulting in a decrease in the DC motor's lifespan. Therefore, it is important to reduce this effect on actuator. This leads to the effective adjustment of nested SMCFz gains, resulting in a significant reduction of the magnitude of chattering effect in the control signal. The key points of this paper are listed below:

• Nested sliding surfaces were designed in such a way that after sliding motion, the position and velocity of the servomechanism exhibit exponential behavior. As far as the authors are aware, the proposed nested sliding surface has not been reported in the literature to date.

• One of the contributions of this work is the integration of a heuristic if–then control structure, which constitutes the foundation of fuzzy control. This approach is further enhanced through the use of ANFIS, providing adaptive capabilities, and has been validated through experimental implementation.

• A neuro-fuzzy scheme was designed to ensure a smooth transition of control gains across nested sliding surfaces.

• The proposed control method combines Nested Sliding Mode Control and neuro-fuzzy control (SMCFz) features to achieve adequate trajectory performance while reducing the magnitude of the chattering effect on the control signal.

Furthermore, a comparative study is being conducted between a PID control and the Nested-SMC with gain adjustment based on the servo position error (SMCif). The proposed control performance is tested under different position set-points of the servomechanism. Here, the performance analysis of the controller under consideration is carried out using common error criteria metrics, such as the Integral Square Error (ISE), Integral Time-weighted Square Error (ITSE), Integral Absolute Error (IAE), and Integral Time-weighted Absolute Error (ITAE).

The paper outline is as follows: In Section 2, the dynamic model of the servomechanism, some sliding mode control preliminaries, and the problem statement are discussed. The development of SMC with nested surfaces for robust position and servomechanism velocity regulation is discussed in Section 3. Section 4 presents the design of intelligent control for adjusting nested control gains using a neuro-fuzzy scheme. The next section presents the experimental test of the proposed control algorithm, along with a comparative study with PID and SMC controllers. An error performance analysis is also included in this section. Finally, concluding remarks are presented in Section 5.

2. Preliminaries and problem statement

The servomechanism being discussed is a pendulum driven by a DC motor. The dynamic behavior of the DC motor is described by differential equations that account for the electrical and mechanical processes involved (Chapman, 2012). Fig. 1 depicts the servomechanism under consideration. Table 1 describes the system components along with their characteristics.

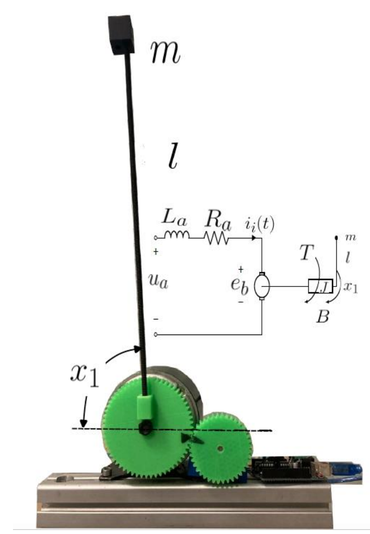

Fig. 1: Experimental environment for the servomechanism system.

Table 1: Characteristics of the servomechanism system.

Components	Characteristics
DC Motor	12VDC, 250W, 2650RPM, 1.5 A nominal.
Sensor	10kΩ Precision Multi-turn Potentiometer.
Microcontroller	Arduino UNO
Motor driver	BTS7960H
module	45V, 40A, Mosfet technology

The mathematical model of the servomechanism is derived from Newton's equations and Kirchhoff's laws (Poznyak, 2021). As a result, the state space representation of the nonlinear system in a conventional form is:

$$\begin{aligned} \dot{x} &= f(x) + \mathbf{B}u, \\ y &= \mathbf{C}x, \quad x(0) = x_0, \end{aligned} \tag{1}$$

where $x \in \mathbb{R}^3$ is the system state, and it deals with the angular position, angular velocity of the pendulum, and the armature current of the DC-motor as x_1, x_2, and x_3 respectively. The control input is denoted as $u \subset \mathcal{U} \in \mathbb{R}$ and it is refers to the armature voltage of the DC-motor. The nonlinear function associated to the system dynamics is represented as $f: \mathbb{R}^3 \to \mathbb{R}^3$, and it is assumed that $f(0) = 0$. The vector $\mathbf{B} \in \mathbb{R}^3$ is called the control vector, and the system output is given by the measurement of position of the servomechanism. In this way, the state representation of the servomechanism is expressed as:

$$\begin{aligned} \dot{x} &= \begin{bmatrix} \dot{x}_1 \\ \dot{x}_2 \\ \dot{x}_3 \end{bmatrix}, \; f(x) = \begin{bmatrix} x_2 \\ \frac{g}{l}\sin(x_1) - \frac{B}{ml}x_2 + \frac{k_i}{ml}x_3 \\ -\frac{k_b}{L_a}x_2 - \frac{R_a}{L_a}x_3 \end{bmatrix}, \\ \mathbf{B} &= \begin{bmatrix} 0 \\ 0 \\ \frac{1}{L_a} \end{bmatrix}, \; \mathbf{C} = [1 \quad 0 \quad 0]. \end{aligned} \tag{2}$$

The parameters of the servomechanism are given in the Table 2. Notice that in the considered system, the armature current of the DC-motor is not available to be measured, however, for control design purposes, the current x_3 consumed by the DC motor is constrained as $\| x_3 \| \leq \gamma = 1.5 \; A$. This bound is determined based on the nominal current value specified in the motor's datasheet. The control problem for this system deals with regulating the position and velocity of the pendulum, where the control input excitation is a DC voltage

Table 2: Engine parameter coefficients

Variable	Descriptions	Value	Units
B	Friction coefficient	0.1	$\frac{N \cdot m}{Rad}$
g	Gravitational acceleration	9.81	$\frac{m}{s^2}$
k_i	Motor sensitivity constant	0.01	$\frac{N \cdot m}{A}$
k_b	Back EMF constant	0.01	$\frac{V \cdot s}{rad}$
l	Length of the pendulum	0.4	m
L_a	Armature inductance	0.05	H
m	Mass of the pendulum	0.3	Kg
R_a	Armature resistance	2	Ω

To regulate the servomotor at different setpoints, the control design for the regulation problem based on the system's linear model needs to be designed for each setpoint. Hence, it is believed that a control design based on the nonlinear model is feasible. Since the dynamic system involves uncertain but bounded dynamics, such as the system's current, designing a robust control based on Sliding Mode Control is appropriate. On the other hand, since the system has a relative degree of 3, the design of an SMC needs to be of a higher-order SMC type. The magnitude of the chattering effect needs to be minimized to prevent damage to the actuator. So, the problem can be stated as follows.

Problem description: Our current challenge involves designing a high-order SMC (in this case, nested-SMC) to regulate the angular position and velocity at various set-points in the presence of uncertain dynamics of the servomechanical system. To this end, in this paper, the trajectory error is considered as, $e = x - x^d$ where x^d deals with the wanted set-point of the state x, i.e.

$$e_1 = x_1 - x_1^d,\ e_2 = x_2 - x_2^d,\ e_3 = x_3 - x_3^d. \tag{3}$$

where x_1^d denotes the desired pendulum position, x_2^d the desired pendulum angular velocity, and x_3^d the desired armature electric current. Since the current is assumed to be unavailable for measurement, the error term e_3 is not considered in the design of the sliding surface. Accordingly, the problem statement focuses on the following relationship:

$$\lim_{t\to\infty} e_1 = 0,\ \ \lim_{t\to\infty} e_2 = 0. \tag{4}$$

Thus, the control scheme must be applicable under any initial condition. In addition, an intelligent reasoning system based on ANFIS is introduced to reduce the chattering effect magnitude on the actuator. The trajectories are expected to converge exponentially. In the following section, a control system is developed using the nested surfaces technique within SMC.

3. Design a nested sliding surface control for Sliding Mode Control (SMC)

The issue arises from the robust regulation of the position and angular velocity of the pendulum, where $x_2 = \dot{x}_1$. Now, consider a conventional asymptotic sliding surface:

$$\sigma = e_2 + \lambda_1 e_1, \qquad \lambda_1(t) = \lambda_1 \quad \lambda_1 > 0. \tag{5}$$

with λ_1 is a decay gain. If the sliding motion occurs in time $t \le T_1$, then the angular position and velocity converge exponential form, see for instance (Levant, 2003; Fridman et al., 2015; Shtessel et al., 2014). The previous statement pertains to regulating the position and velocity of the pendulum. However, the dynamics of this surface do not involve the control input u, then the sliding motion is compromised. In this sense, propose another sliding mode surface that depends on the previous one, as follows:

$$\delta = \dot{\sigma} + \lambda_2 \sigma, \qquad \lambda_2(t) = \lambda_2 \quad \lambda_2 > 0. \tag{6}$$

The concept of nested equations in sliding modes is discussed in (Huerta-Avila et al., 2007; Miranda-Villatoro et al., 2017). The concept of nesting is interpreted in different ways, like repeating the same equation n times. For instance, in asymptotic SMC, a sliding surface relies on an error function to produce a desired solution where $\dot{\sigma} = \dot{e}_2 + \lambda_1 \dot{e}_1$ and $\ddot{\sigma} = \ddot{e}_2 + \lambda_1 \ddot{e}_1$. Furthermore, in (Samo et al., 2020; Kang et al.,2025), the authors use integrals to derive the equation $\sigma = e - \int_0^t \lambda e d\tau$. By differentiating twice, they arrive at the expressions $\dot{\sigma} = \dot{e} - \lambda e, \ddot{\sigma} = \ddot{e} - \lambda \dot{e}$. In contrast, this work involves two equations of the sliding surfaces (5) and (6), resulting in a complete differential equation. Furthermore, it includes two associated parameters, λ_1 and λ_2, in an equation of the form $\dot{\delta} = \ddot{e}_2 + \dot{e}_2(\lambda_1 + \lambda_2) + e_2 \lambda_1$. This concept is associated with a nested surface.

So, consider the temporal derivative of the sliding surfaces (5) and (6) along the trajectories of the system (1)-(2), next statement is obtained:

$$\dot{\sigma} = \dot{e}_2 + \lambda_1 e_2 + \dot{\lambda}_1 e_1 \tag{7}$$

where $e_2 = x_2 - x_2^d$, and $\dot{e}_2 = \dot{x}_2$, from the state variable, we obtain:

$$\dot{e}_2 = \frac{g}{l}\sin(x_1) - \frac{B}{ml}x_2 + \frac{k_i}{ml}x_3,$$

rewriting (7) with the system dynamics yields

$$\dot{\sigma} = \frac{g}{l}\sin(x_1) - \frac{B}{ml}x_2 + \frac{k_i}{ml}x_3 + \lambda_1 x_2 + \dot{\lambda}_1 x_1,$$

in the same way that is derived (6)

$$\dot{\delta} = \ddot{\sigma} + \lambda_2\dot{\sigma}, \tag{8}$$

substituting (7) into (8)

$$\dot{\delta} = \ddot{e}_2 + \dot{e}_2(\lambda_1 + \lambda_2) + e_2\left(2\dot{\lambda}_1 + \dot{\lambda}_2 + \lambda_1\lambda_2\right) + e_1\left(\ddot{\lambda}_1 + \lambda_1\dot{\lambda}_2 + \lambda_2\dot{\lambda}_1\right). \tag{9}$$

Since λ_1 and λ_2 are smooth functions, it is said that $\dot{\lambda}_1$ and $\dot{\lambda}_2$ are bounded, $2\dot{\lambda}_1 + \dot{\lambda}_2 = \varphi$ and $\ddot{\lambda}_1 + \lambda_1\dot{\lambda}_2 + \lambda_2\dot{\lambda}_1 = \xi$, rewriting

$$\dot{\delta} = \ddot{e}_2 + \dot{e}_2(\lambda_1 + \lambda_2) + e_2(\varphi + \lambda_1\lambda_2) + e_1\xi \tag{10}$$

$$\dot{\delta} = \ddot{x}_2 + \dot{x}_2(\lambda_1 + \lambda_2) + x_2(\varphi + \lambda_1\lambda_2) + x_1\xi$$

$$\begin{aligned}\dot{\delta} = {} & \frac{g}{l}\cos(x_1) - \frac{B}{ml}\dot{x}_2 + \frac{k_i K_b}{mlL_a}x_2 - \frac{k_i R_a}{mlL_a}x_3 + \\ & \frac{k_i}{mlL_a}u + (\lambda_1 + \lambda_2)(\frac{g}{l}\sin(x_1)) - \frac{B}{ml}x_2 - \\ & \frac{k_i}{ml}x_3 + x_2(\varphi + \lambda_1\lambda_2) + x_1\xi.\end{aligned} \tag{11}$$

By considering the control action in the form $u = u_1 + u_2$, where u_1 represents the control in sliding modes and u_2 is an equivalent control in the form

$$\begin{aligned} u_1 = {} & -\frac{mlL_a}{k_i}\rho\mathrm{sign}(\delta), \\ u_2 = {} & -\frac{mlL_a}{k_i}[\frac{g}{l}\cos(x_1) - \frac{B}{ml}\dot{x}_2 + \frac{k_i K_b}{mlL_a}x_2 - \\ & \frac{k_i R_a}{mlL_a}x_3 + (\lambda_1 + \lambda_2)(\frac{g}{l}\sin(x_1) - \\ & \frac{B}{ml}x_2 - \frac{k_i}{ml}x_3 + x_2(\varphi + \lambda_1\lambda_2) + x_1\xi],\end{aligned} \tag{12}$$

with

$$\mathrm{sign}(\delta) = \frac{|\delta|}{\delta} = \begin{cases} \rho & \delta > 0 \\ -\rho & \delta < 0 \\ (-\rho, \rho) & \delta = 0 \end{cases} \tag{13}$$

applying the control law (12) in (11), can be rewritten as

$$\dot{\delta} = \rho\mathrm{sign}(\delta). \tag{14}$$

However, since x_3 is not available in a measurable form and is proposed to be bounded due to the motor's physical parameters, this is considered negligible. Therefore, the control u_2 and the gain ρ are selected as:

$$u_2 = -\frac{mlL_a}{k_i}\left[\frac{g}{l}\cos(x_1) - \frac{B}{ml}\dot{x}_2 + \frac{k_i k_b}{mlL_a}x_2 + (\lambda_1 + \lambda_2)\left(\frac{g}{l}\sin(x_1)\right) - \frac{B}{ml}\,x_2 + x_2\,(\varphi + \lambda_1\,\lambda_2\,) + x_1\,\xi\right] \tag{15}$$

The parameter ρ is a gain that mitigates the effects of uncertain dynamics and external disturbances. And $\dot{\delta} \leq \rho\mathrm{sign}(\delta)$.

$$\rho = \frac{mlL_a}{k_i}\left[\frac{k_i R_a}{mlL_a} - \frac{k_i}{ml}\right]\gamma = 2.98.$$

Consequently, the magnitude of ρ directly influences the amplitude of the chattering produced on the control signal. It should be noted that the control action is defined in (14). To further analyze system stability, introduce the following Lyapunov energy function. (Polyakov & Fridman., 2014):

$$V(\delta) = \frac{1}{2}\delta^2, \tag{16}$$

to ensure convergence within a finite time, consider $\rho - \epsilon = \alpha$ if $\alpha > 0 \Rightarrow \rho = \alpha + \epsilon$, to $\epsilon \ll 1$. The time variations of this function along the trajectories (14) yields

$$\dot{V}(\delta) = \delta\dot{\delta} \leq -\alpha\delta \text{sign}(\delta) = -\rho\delta\frac{|\delta|}{\delta} \leq -\alpha|\delta|, \tag{17}$$

it is important to note that $|\delta| = \sqrt{\delta^2}$, then (17) is obtained as,

$$\dot{V}(\delta) \leq -\rho\sqrt{2}V^{\frac{1}{2}}(\delta). \tag{18}$$

The worst case of previous differential inequality is given by

$$\frac{d}{dt}V(\delta) = -\alpha\sqrt{2}V^{\frac{1}{2}}(\delta) \tag{19}$$

the solution of the previous differential equation in time $\tau \in [t_0, t]$ yields:

$$V(\delta)^{-\frac{1}{2}}dV(\delta) = -\alpha\sqrt{2}dt$$

$$\int_{t_0}^{t} V(\delta)^{-\frac{1}{2}}\frac{d}{d\tau}V(\delta)d\tau = -\alpha\sqrt{2}\int_{t_0}^{t} d\tau$$

$$2V(\delta)^{\frac{1}{2}}|_{t_0}^{t} = -\alpha\sqrt{2}\tau|_{t_0}^{t},$$

which means that the solution is given by next statement

$$V^{\frac{1}{2}}\big(\delta(t)\big) = V^{\frac{1}{2}}(\delta_0) - \alpha\frac{1}{\sqrt{2}}(t - t_0). \tag{20}$$

So, from the comparison lemma, if previous solution is fulfilled, the next statement holds

$$V^{\frac{1}{2}}(\delta) \leq V^{\frac{1}{2}}(\delta_0) - \frac{\alpha}{\sqrt{2}}(t - t_0),$$

and for the worst case, the convergence to reach zero at

$$0 = V^{\frac{1}{2}}(\delta_0) - \frac{\alpha}{\sqrt{2}}(t - t_0),$$

Finally, the sliding motion occurs in time

$$t \in \left[t, \frac{\sqrt{2}}{\alpha}V^{\frac{1}{2}}(x_0) + t_0\right]. \tag{21}$$

The sliding surface δ converges to zero. Therefore, the next statement holds.

$$\dot{\sigma} = -\lambda_2 \sigma\sigma(t) = \sigma_0 e^{-\lambda_2 (t-T_1)}. \tag{22}$$

It is observed that the sliding surface converges to zero in finite time, as shown in the analysis using the first Lyapunov method (Khalil, 2004). The time constant for the stepped convergence is defined as $T = \lambda_2^{-1}$. By considering ten time constants in the decreasing exponential, the response reaches 99.99% of the final value. So after time $T_2 = T_1 + 10 \times T$, it is considered that the sliding motion $\sigma = 0$ is fulfilled. This means that after time T_2, the next statement holds:

$$\dot{e}_1 = -\lambda_1 e_1. \tag{23}$$

As shown in equation (22), in this case, the angular position error exponentially converges to zero. The same applies to the angular velocity error. This implies that exponential stability is achieved for the position and angular velocity of the servomechanism. However, due to the form of the control signal u_1, there is no guarantee that chattering in its magnitude will be reduced. Based on the information provided and to the best of the author's knowledge, the magnitude of chattering in the control signal after sliding motion depends on the gain ρ of the sliding mode control u_1. Furthermore, the trajectories performance depends on the values of λ_1 and λ_2, which represent the gains of the sliding surfaces designed in the robust control. Notice that λ_1 represents the convergence rate when the corresponding sliding surface is zero, resulting in the position error trajectory exhibiting exponential decay. Similarly, λ_2 influences the convergence of the sliding surface associated with λ_1, which also leads to trajectories with exponential decay. Within the proposed control scheme, the gain ρ plays a crucial role in mitigating the effects of disturbances and uncertain dynamics. As established in sliding mode theory, the magnitude of ρ directly affects both the control action and the resulting chattering phenomenon. By adjusting ρ as $\delta \to 0$, the magnitude of the chattering can be effectively reduced.

The aggregate dynamic uncertainty $\Delta f(x,t)$ and the unmodeled external disturbances d(t) are bounded such that $\|\Delta f(t,x) + d(t)\| \leq D_{max}$, where $D_{max} > 0$ is a known or estimable constant. This was obtained by considering the worst-case motor voltage scenario (see Table 1), which also includes friction coefficients, changes in load torque, and maximum expected disturbances during experimental operation.

Assumption 1: The overall uncertainty term $\delta(x,t)$, which includes parametric variations and unmodeled disturbances, is bounded by a positive constant D_{max}, such that $\|\Delta f(t,x) + d(t)\| \leq D_{max} < \infty$. Based on the maximum motor torque limits (see Table 1), D_{max}, was proposed to be 200. Consequently, the control switching gain was selected as having a range $\rho < 200$, strictly satisfying the reachability condition during experimental testing.

Therefore, the proposed approach suggests tuning this gain through an error-dependent function, guided by expert knowledge. This serves as motivation to adjust control gains using intelligent control tools such as ANFIS. In this way, a feedback control system is proposed, as depicted in Fig. 2.

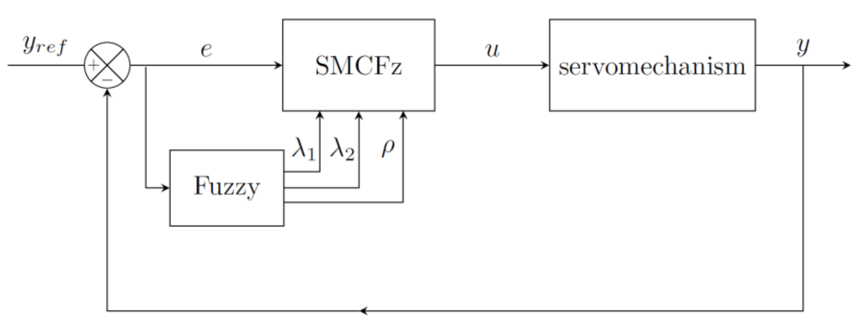

Fig. 2: Proposed block diagram.

After designing the control system using nested surfaces, it is suggested to adjust the parameters based on the error using the Fuzzy approach.

3 Nested SMC control design, tuning the parameters with fuzzy logic (SMCFz)

The aim of this section is to reduce the magnitude of the chattering effects and enhance convergence towards the desired set-point by intelligently adjusting parameters λ_1, λ_2, and ρ in equations (5), (6), and (12) when the system is in sliding motion. During the sliding motion, a chattering effect occurs, and its reduction depends on the coefficient associated with the sign function in the sliding control. Assigning a high gain ρ increases the chattering amplitude. To mitigate this effect, it is suggested to adjust the gain ρ using fuzzy control, based on the magnitude of the position error. A small position error results in a small gain ρ, which helps reduce the amplitude of chattering. This can be confirmed through a stability test that assumes the presence of disturbances or dynamic uncertainties, thereby considering the worst-case scenario. In the absence of such perturbations or uncertainties, there is no need for ρ to have a high magnitude. When $0 < \rho \ll 1$, the magnitude of chattering is significantly reduced. This behavior can be observed in the stability test by removing the constraint and assuming that $\alpha = \epsilon$. A switching procedure based on conditional if-then rules type Takagi-Sugeno is proposed to generate an inference based on heuristic knowledge. The proposed control scheme is depicted in Fig. 3. In order to gain a deeper understanding, several experiments were conducted on the system. One of them involved programming a simple conditional statement (*if*) simple conditional statement, for decision-making in the control strategy and to obtain the SMCif tuning parameters shown in Table 3.

Table 3: Parameters Tuned with the error conditional, (SMCif) $\epsilon = 0.039$.

error	ρ	λ_1	λ_2
$e > \epsilon$	20	1	20
$e \leq \epsilon$	1	0.5	1

This helped to understand the chaotic behaviour of the system, which led to the development of three fuzzy models with 5 rules each. Table 5 shows the parameters of the premises with Gaussian membership functions and zero-order consequent.

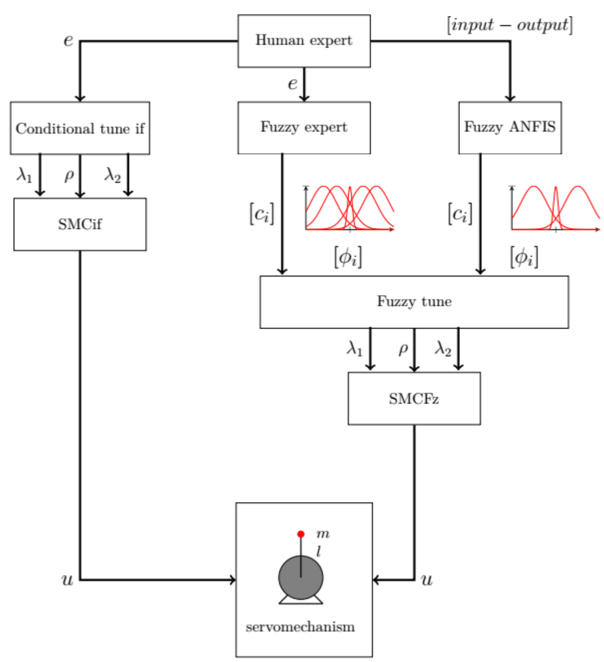

Figure 3: Expert system for optimization of parameters SMCFz.

The parameters of the assumptions are displayed using Gaussian membership functions and a zero-order consequent. human expertise from the SMCif experiment was utilized to establish the suitable parameters for a model with fuzzy rules. As the model will be tested in real-time, it is important to reduce the number of controller parameters. The expert's initial proposal, which included 5 rules, was optimized to 3 rules. Table 6 depicts the improved parameters for a comparable fuzzy system response achieved through the ANFIS algorithm (Jang, 1993).

Table 4: Parameters for learning in Fuzzy ANFIS

Generate FIS…		**Train FIS**	
INPUT		Optim. Method	Hybrid
Number of MFs	3	Error Tolerance	0.01
MF Type	Gaussmf	Epochs:	50
OUTPUT			
MF Type	constant		

In the ANFIS interface of Matlab, a learning phase is conducted using the data presented in Table 4 together with input-output experimental measurements for each of the three parameters: $[e, \rho]$, $[e, \lambda_1]$, and $[e, \lambda_2]$. These pairs are derived from multiple experiments conducted with the conditional SMCif. They led to an enhanced fuzzy model consisting of 3 rules, which reduced the number of parameters defined in the fuzzy models. The functions being considered in the design are a type of normal fuzzy set within the universe of discourse in the Gaussian membership form:

$$f(e, \phi_i, c_i) = exp\left(\frac{e-c_i}{\sqrt{2}\phi_i}\right)^2, \tag{24}$$

where c_i and ϕ_i, are the centroid and the dispersion of the $i-th$ membership function, with $i = 1, \cdots, R$ rules and e is the input variable. In Equation (24), the variable e represents the position error of the system in closed-loop control. During the tuning phase by the human expert, five linguistic categories are proposed to define the error e: a large positive error (eLP), a large negative error (eLN), a small positive error (eSP), a small negative error (eSN), and zero error (eC). To automatically adjust each parameter λ_1, λ_2, and ρ, five zero-order Sugeno fuzzy rules were proposed in Equation (25).

$$R_i: If\ e(k)\ is\ A_i, then\ Parameter = S_i. \tag{25}$$

Table 5: Parameter vectors from human expertise.

Parameter	**premises**		**consequents**
$i = 1,\ldots,5$	c_i	ϕ_i	S_i
λ_1	[-6.14 -1 0 1 6.14]	[2 0.5 0.1 0.5 2]	[200 20 1 20 200]
λ_2	[-6.14 -1 0 1 6.14]	[2 0.5 0.1 0.5 2]	[250 20 1 20 250]
ρ	[-6.14 -1 0 1 6.14]	[2 0.5 0.1 0.5 2]	[5000 20 2 20 5000]

Table 6: Parameter vectors from ANFIS.

Parameter	**premises**		**consequent**
$i = 1,\ldots,3$	c_i	ϕ_i	S_i
λ_1	[-4 0 4]	[1.699 0.699 1.699]	[700 3.99 700]
λ_2	[-4 0 4]	[1.699 0.699 1.699]	[100 1 100]
ρ	[-4 0 4]	[1.699 0.699 1.699]	[150 1 150]

To obtain the output of each *Parameter*(λ_1, λ_2, and ρ), next weighted averages on the defuzzification procedure were used

$$Parameter = \frac{\sum_{i=1}^{R} \mu_{A_i}(e(k)) s_i}{\sum_{i=1}^{R} \mu_{A_i}(e(k))}. \tag{26}$$

4. Experimental results

The servomechanism comprises a microcontroller, an H-bridge, a variable electric-resistor as a motor shaft position sensor, and a motor linked to a pendulum mechanically. After placing the three control programs PID, SMCif, SMCFz, and SMCFz ANFIS inside the microcontroller, the execution time was measured using the "millis()" instruction. The times obtained were 7.8 ms, 7.3 ms, 12.3 ms, and 8.4 ms, respectively. Observe a decrease in execution time in the hybrid SMCFz control when tuned with ANFIS. It is worth mentioning that the ANFIS training was conducted offline in MATLAB. Next, a comparative study was conducted on three different control methods (PID, SMCif, and SMCFz) tested in the servomechanism. The inclusion of the Ziegler–Nichols tuned PID controller is motivated by its widespread use in industrial applications. Although such comparisons may appear limited, evaluating different control strategies can provide valuable insights when selecting the most appropriate approach for a given plant. To ensure fairness in the comparative analysis, the proposed SMCFz was also benchmarked against its conditional counterpart.

4.1 Control PID

The PID controller

$$u(t) = k_p e(t) + k_i \int e(t)dt + k_d \frac{de(t)}{dt}, \tag{27}$$

was implemented in the microcontroller. This scheme was discretized using the Euler method approximation (Franklin et al., 1998),

$$u[k] = u[k-1] + (K_p + TsK_i + K_d/Ts)ek - (K_p + (2K_d)/Ts)e[k-1] + (K_d/Ts)e[k-2].$$

During the experiments, a sampling time of *Ts* = 0.01 seconds was used. The parameters k_p, k_i, and k_d represent the proportional, integral, and derivative constants, respectively. These values were determined using the first Ziegler-Nichols closed-loop method (Sekara et al., 2010). The obtained values are: $k_p = 1551$, $k_i = 13.5$, and $k_d = 0.1$. The initial condition is $x_1(0) = \pi/2$ radians, and the desired position is 0 radians. Three experiments were conducted with different control set-points at 0, 0.2, and 0.4 radians (0, 11.5, and 23 degrees), respectively. It is worth mentioning that the PID control algorithm was tuned using the Ziegler-Nichols method with additional fine-tuning. This does not imply that there is a specific set of control gains for the PID that guarantee superior performance.

4.2 Nested Sliding Mode Control with conditional (SMCif)

As mentioned in the problem statement, sliding mode control is a technique used to achieve robust control. However, the challenge lies in addressing issues related to energy consumption and wear of actuators, i.e. reduce the magnitude of the chattering effect. First, the coefficients λ_1, λ_2, and ρ in equations (5), (6), and (12) were initially proposed heuristically in the simulation. By carrying out a variety of experiments, the values were refined to effectively control the servomechanism. Various experiments were carried out on a real servomechanism system, where parameters were adjusted based on the response and reduced when the error approached zero. For instance, placing the controlled variable near the set-point greatly reduces the magnitude of the chattering, allowing its value to be adjusted according to a condition.

$$\begin{aligned} &If e(k) > 0.039, \text{then } Parameter = \text{constant big}, \\ &If e(k) \leq 0.039, \text{then } Parameter = \text{constant small}. \end{aligned} \tag{29}$$

In practice, the parameters were determined based on Table 3.

4.3 Robust control, Nested Sliding Mode Control Fuzzy (SMCFz)

In this case, a fuzzy inference system was developed to adjust the parameters λ_1, λ_2, and ρ. The control error is the linguistic variable which requires the inference and defuzzification process to be carried out at each sampling time. The SMCif serves as the foundation for enhancing the obtained results through the use of intelligent adaptive neuro-fuzzy control. This allows for the necessary expertise to manually adjust the coefficients c_i, ϕ_i and S_i during programming on the microcontroller. Additionally, it is important to compare the two methods of tuning constants using fuzzy logic.

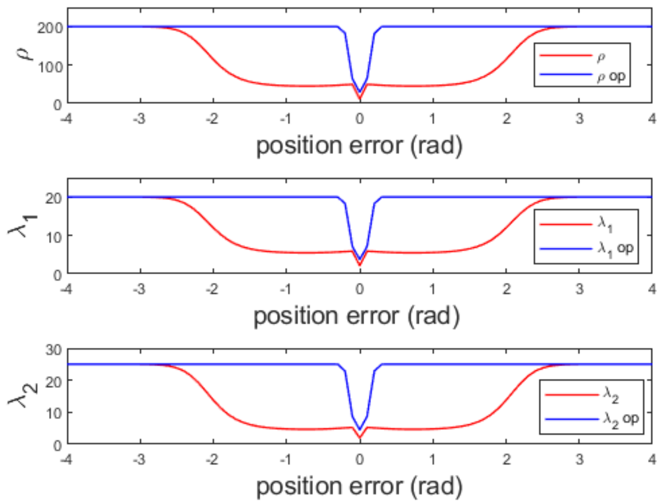

Fig. 4: Curves of parameters learned by the expert and ANFIS $\rho, \lambda_1, \lambda_2$ and (ρ, λ_1 and λ_2) optimal, respectively.

The first method involves incorporating human experience by defining 5 rule bases and 5 membership functions. The results are depicted by the red line in Fig. 4, which shows graphs for ρ, λ_1, and λ_2. The second graph was created using Matlab's ANFIS tool. The number of rules was reduced, as shown by the blue line in Fig. 4, which represents the variables ρ_{op}, λ_{1op}, and λ_{2op}. Optimizing the number of rules and their corresponding membership functions helps the SMC control parameters maintain robustness as they approach zero asymptotically. It is important to note that the constants ρ, λ_1, and λ_2 can be reduced by adjusting the dispersion or width of the Gaussian function. This will help reduce noise as the system reaches the desired reference, due to the natural effect of chattering. In practice, the constants behaved asymptotically as depicted in Fig. 8, resembling the optimization graphs in Fig. 4.

4.4 Numerical test

This section presents the results derived from the proposed control scheme. All results in this section are related to the experimental platform exposed in Figure 1, with the system parameters indicated in Table 1. The results presented in Figures 5, 6, 7, and 8 are derived from numerous real experiments conducted under various conditions, including changes in the input voltage of a DC motor and adjustments to the initial states, among other factors. The results obtained are highly consistent with those reported. The initial conditions for all experiments are $x_1(0) = \pi/2$, $x_2(0) = 0$, and $x_3(0) = 0$, which represent the initial position, the initial angular velocity of the pendulum, and the initial electrical current of the motor, respectively. The experimental results are shown in Figures 5-7. The red line represents the PID, the magenta line represents the SMCif, and the blue line represents the SMCFz. Fig. 5 shows the results of the servomechanism with a setpoint of 0 radians, Fig. 6 illustrates the experiment when the setpoint is at 0.2, while Fig. 7 presents the test when the setpoint is at 0.4 radians.

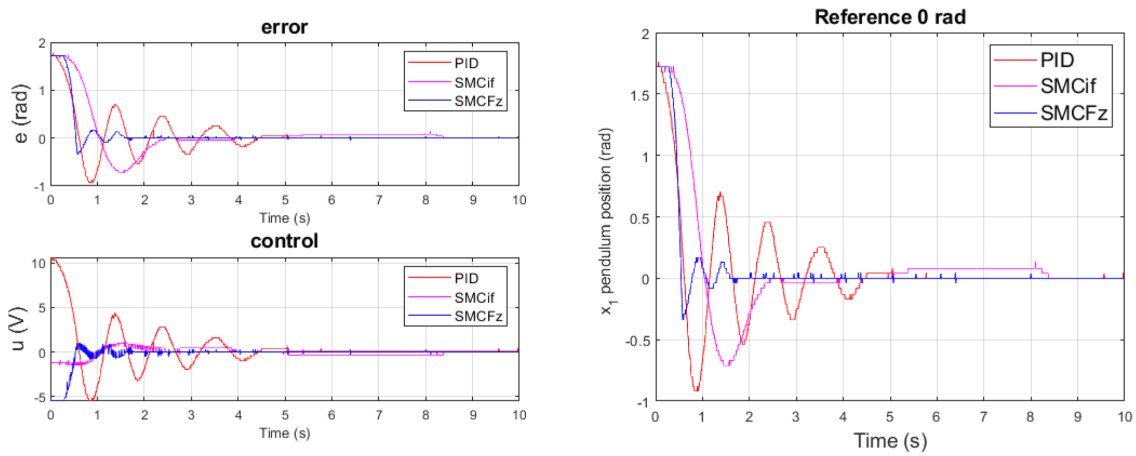

Fig. 5: Pendulum position error and control signal with set-point at 0 rad.

In all three cases analyzed, it is clear that the angular position of the servomechanism under SMCFz control shows improved performance, such as reduced settling time, along with other parameters listed in Table 7. In fact, SMCFz settles in less than 4 seconds. Furthermore, it is visually apparent that the generated control signal consumes less energy compared to the other control actions. The second-best performing controller is the SMCif, while the PID controller still exhibits lower performance. The above is supported by a steady-state error analysis with a 2% criterion and an energy analysis of the control signal, as shown in Table 7. Furthermore, it can also be observed that in terms of RMS error, the control that performs best is SMCFz, where the magnitude of this error is much lower than in the other algorithms. Chattering Mitigation: While the conventional SMC displayed significant chattering (high), the proposed implementation in the SMCFz effectively reduced these high-frequency oscillations (reduced). Although the PID controller does not exhibit chatter (no), its slow response speed and higher error justify adopting the SMCFz hybrid scheme as the optimal solution for robust plant control.

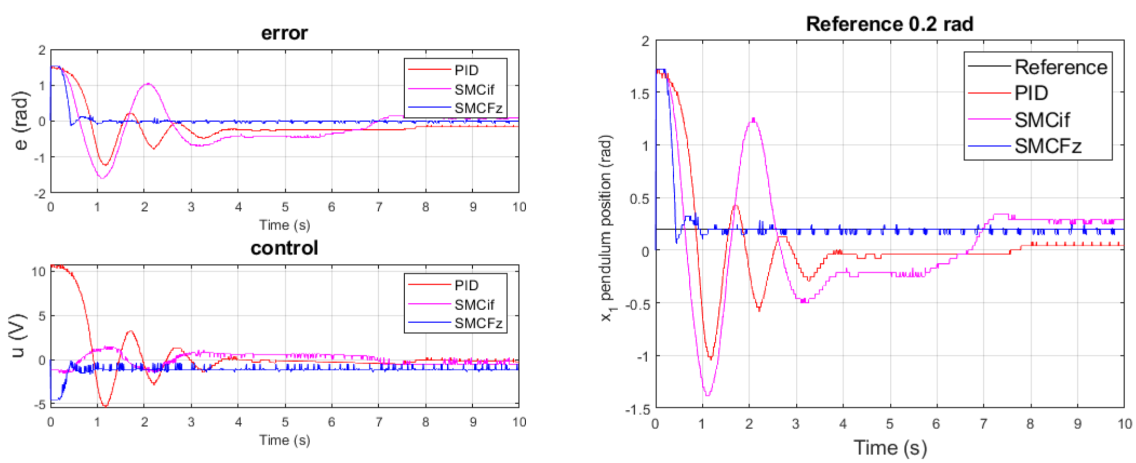

Fig. 6: Numerical results of the servomechanism with set-point at 0.2 rad.

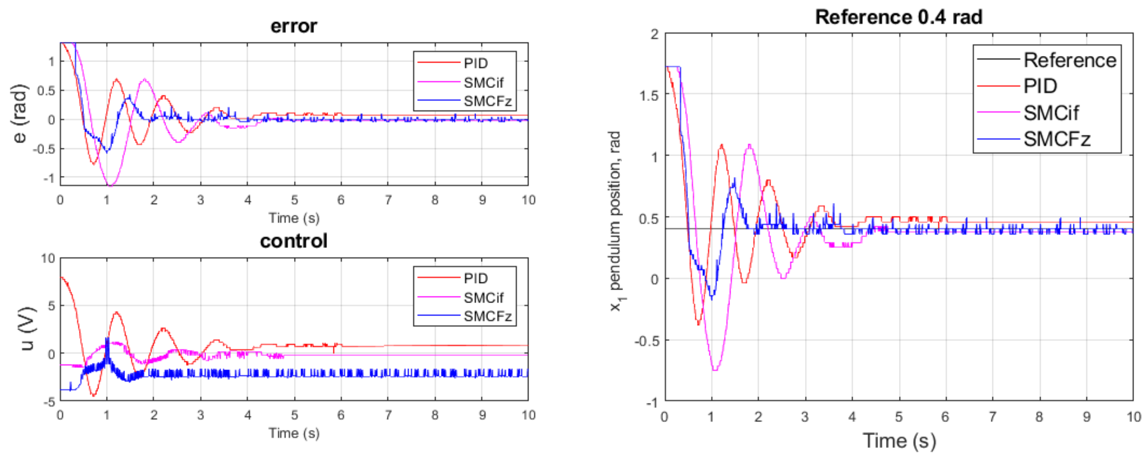

Fig. 7: Servomechanism numerical test at set-point in 0.4 rad.

Table 7: Comparative study for considered controllers.

	PID			SMCif			SMCFz		
Reference (rad)	0	0.2	0.4	0	0.2	0.4	0	0.2	0.4
e_{ss} (rad)	0	0.1	0.05	0	0.04	0.1	0.01	0.02	0.03
e_{rms}	0.51	0.6	0.37	0.61	0.75	0.51	0.35	0.34	0.36
t_s(s)	5.2	19	14	8.5	10	5	1.8	2.5	4
Energy= $\lim_{T-\infty}\frac{1}{T}\int_0^T u^2\,dt\ \ (v^2s)$	600	800	300	1500	1900	1300	120	90	180
Chattering effect	no	no	no	high	high	high	reduced	reduced	reduced

On the other hand, to achieve the best trajectory performance, it is important to consider error criteria such as ISE, IAE, ITSE, and ITAE. The analysis presented in Table 8 supports this statement.

Table 8: Error-integral performance indexes

$x_1(0) = \pi/2$	PID			SMCif			SMCFz		
Reference (rad)	0	0.2	0.4	0	0.2	0.4	0	0.2	0.4
ISE	157	217	83	225	33	157	124	70	77
IAE	186	274	144	196	385	193	89	61	98
ITSE	10k	24k	6k	11k	56k	12k	2.7k	1.2k	2.7k
ITAE	24k	55k	22k	19k	91k	25k	3.3k	3.1k	8.2k

The algorithm, based on ANFIS, generates the adjustment parameters ρ, λ_1, and λ_2. These parameters gradually decrease using Gaussian-type membership functions until they reach a constant value as the angular position error of the servomechanism arrives at zero. The effect of parameter adjustment is depicted for the three cases in Fig. 8.

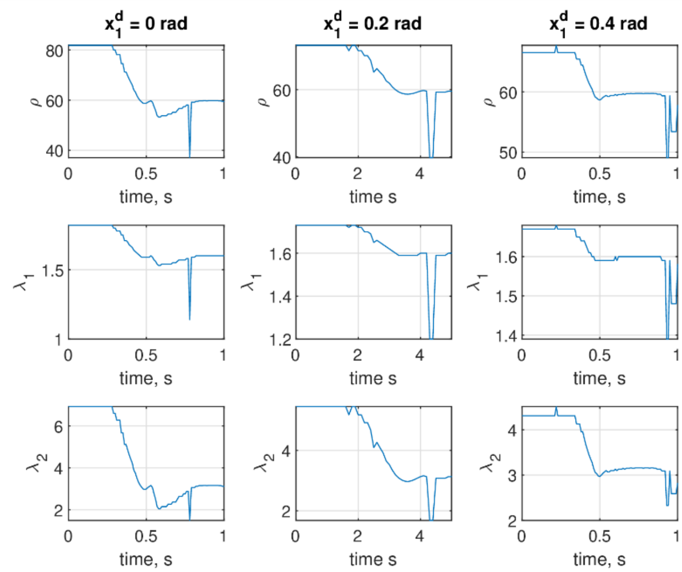

Figure 8: Parameter adjustment ρ, λ_1(t), $\lambda_2(t)$ for the SMCFz.

5 Conclusions

This paper presents the design of a robust intelligent control system that can handle external disturbances and dynamic uncertainties. To achieve this, a method was developed using nested sliding surfaces with neurofuzzy adaptation of control gains. This method allowed for maintaining robust characteristics without putting strain on the actuators. Furthermore, it allows for improved response and stabilization. Similarly, using ANFIS for tuning allows for a smooth adjustment of the parameters ρ, λ_1, and λ_2 based on the error signal of angular position, which contributes to reduce the magnitude of the chattering effect in the control signal. This control system was successfully implemented in a servomechanism to regulate its position and speed through a voltage signal, which indicates considerable feasibility for implementing this methodology in various industrial processes. The effectiveness of the designed controller was first evaluated in a comparative study against PID controllers and conditional fuzzy controllers, demonstrating significant improvements in the error criteria ISE, IAE, ITSE, and ITAE. Moreover, the proposed control scheme exhibited enhanced performance in terms of settling time under a 2% criterion, as well as reduced energy consumption. While comparisons with more robust control strategies, such as higher-order sliding mode control or the super-twisting algorithm, are important, these will be addressed in future research.

6 References

Asar, M. F., Elawady, W. M., & Sarhan, A. M. (2019). ANFIS-based an adaptive continuous sliding-mode controller for robot manipulators in operational space. *Multibody System Dynamics, 47*(2), 95–115. https://doi.org/10.1007/s11044-019-09681-5

Aydın, M., & Yakut, O. (2023). Implementation of sliding surface moving ANFIS based sliding mode control to rotary inverted pendulum. *Journal of the Institute of Science and Technology, 13*(2), 1165–1175. https://doi.org/10.21597/jist.1168611

Azar, A. T., & Zhu, Q. (Eds.). (2015). *Advances and applications in sliding mode control systems*. Springer. https://doi.org/10.1007/978-3-319-11173-5

Chapman, S. J. (2012). *Máquinas eléctricas* (5.ª ed.). McGraw-Hill Interamericana.

Cheng, M., Zhou, J., Qian, W., Wang, B., Zhao, C., & Han, P. (2024). Advanced electrical motors and control strategies for high-quality servo systems—A comprehensive review. *Chinese Journal of Electrical Engineering, 10*(1), 63–85. https://doi.org/10.23919/CJEE.2023.000048

Cruz-Ortiz, D., Chairez, I., & Poznyak, A. (2022). Non-singular terminal sliding-mode control for a manipulator robot using a barrier Lyapunov function. *ISA Transactions, 121*, 268–283. https://doi.org/10.1016/j.isatra.2021.04.001

Ertugrul, M., & Kaynak, O. (2000). Neuro sliding mode control of robotic manipulators. *Mechatronics, 10*(1–2), 239–263. https://doi.org/10.1016/S0957-4158(99)00057-4

Feng, Z.-R., Sha, R.-Z., & Ren, Z.-G. (2022). A chattering-reduction sliding mode control algorithm for affine systems with input matrix uncertainty. *IEEE Access, 10*, 58982–58996. https://doi.org/10.1109/ACCESS.2022.3179580

Franklin, G. F., Powell, J. D., & Workman, M. L. (1998). *Digital control of dynamic systems* (3rd ed.). Addison-Wesley.

Fridman, L., Moreno, J. A., Bandyopadhyay, B., Kamal, S., & Chalanga, A. (2015). Continuous nested algorithms: The fifth generation of sliding mode controllers. In X. Yu & M. Ö. Efe (Eds.), *Recent advances in sliding modes: From control to intelligent mechatronics* (pp. 5–35). Springer. https://doi.org/10.1007/978-3-319-18290-2_2

Hamzah, M. K., Al-Azzawi, R. S., Al-Jodah, A., Humaidi, A. J., & Hasan, A. F. (2024). Fuzzy logic-based chattering reduction in sliding mode control of single-link robot using muscle-like actuator. *ICIC Express Letters, 18*(3), 271–283. https://doi.org/10.24507/icicel.18.03.271

Hu, S., Ren, X., Zheng, D., & Chen, Q. (2024). Neural-network-based robust adaptive synchronization and tracking control for multimotor driving servo systems. *IEEE Transactions on Transportation Electrification, 10*(4), 9618–9630. https://doi.org/10.1109/TTE.2024.3374749

Huerta-Avila, H., Loukianov, A. G., & Cañedo, J. (2007). Nested integral sliding modes of large scale power system. In *Proceedings of the 46th IEEE Conference on Decision and Control* (pp. 1993–1998). IEEE. https://doi.org/10.1109/CDC.2007.4434719

Jang, J.-S. R. (1993). ANFIS: Adaptive-network-based fuzzy inference system. *IEEE Transactions on Systems, Man, and Cybernetics, 23*(3), 665–685. https://doi.org/10.1109/21.256541

Kang, Z., Lin, X., Shen, X., Liu, Z., Gao, Y., & Liu, J. (2025). Event-triggered generalised super-twisting sliding mode control for position tracking of PMSMs. *IEEE Transactions on Industrial Informatics, 21*(7), 5701–5711. https://doi.org/10.1109/TII.2025.3556086

Khalil, H. K. (2004). Lyapunov stability. In H. Unbehauen (Ed.), *Control systems, robotics, and automation* (Vol. 12). EOLSS Publishers.

Levant, A. (2003). Higher-order sliding modes, differentiation and output-feedback control. *International Journal of Control, 76*(9–10), 924–941. https://doi.org/10.1080/0020717031000099029

Li, X., Liu, S., Wan, S., & Hong, J. (2020). Active suppression of milling chatter based on LQR-ANFIS. *The International Journal of Advanced Manufacturing Technology, 111*, 2337–2347. https://doi.org/10.1007/s00170-020-06279-6

Li, Z., & Zhai, J. (2024). Fuzzy adaptive super-twisting sliding mode asymptotic tracking control of robotic manipulators. *International Journal of Fuzzy Systems, 26*(1), 34–43. https://doi.org/10.1007/s40815-023-01573-3

Lin, H., Liu, J., Shen, X., Leon, J. I., Vazquez, S., Marquez Alcaide, A., Wu, L., & Franquelo, L. G. (2022). Fuzzy sliding-mode control for three-level NPC AFE rectifiers: A chattering alleviation approach. *IEEE Transactions on Power Electronics, 37*(10), 11704–11715. https://doi.org/10.1109/TPEL.2022.3174064

Miranda-Villatoro, F. A., Castaños, F., & Brogliato, B. (2017). A set-valued nested sliding-mode controller. *IFAC-PapersOnLine, 50*(1), 2971–2976. https://doi.org/10.1016/j.ifacol.2017.08.662

Polyakov, A., & Fridman, L. (2014). Stability notions and Lyapunov functions for sliding mode control systems. *Journal of the Franklin Institute, 351*(4), 1831–1865. https://doi.org/10.1016/j.jfranklin.2014.01.002

Poznyak, A. S. (2021). *Classical and analytical mechanics: Theory, applied examples, and practice*. Elsevier. https://doi.org/10.1016/C2020-0-01741-X

Prieto, P. J., Cazarez-Castro, N. R., Aguilar, L. T., & Cardenas-Maciel, S. L. (2017). Chattering existence and attenuation in fuzzy-based sliding mode control. *Engineering Applications of Artificial Intelligence, 61*, 152–160. https://doi.org/10.1016/j.engappai.2017.03.005

Saihi, L., Berbaoui, B., & Bakou, Y. (2023). Sliding mode of second-order control based on super-twisting ANFIS algorithm of doubly fed induction generator in wind turbines systems with real variable speeds. *Iranian Journal of Science and Technology, Transactions of Electrical Engineering, 47*(2), 473–490. https://doi.org/10.1007/s40998-022-00576-4

Sami, I., Ullah, S., Basit, A., Ullah, N., & Ro, J. S. (2020). Integral super twisting sliding mode based sensorless predictive torque control of induction motor. *IEEE Access, 8*, 186740–186755. https://doi.org/10.1109/ACCESS.2020.3028845

Šekara, T. B., & Mataušek, M. R. (2010). Revisiting the Ziegler–Nichols process dynamics characterization. *Journal of Process Control, 20*(3), 360–363. https://doi.org/10.1016/j.jprocont.2009.08.004

Shtessel, Y., Edwards, C., Fridman, L., & Levant, A. (2014). *Sliding mode control and observation*. Birkhäuser. https://doi.org/10.1007/978-0-8176-4893-0

Utkin, V., & Lee, H. (2006). Chattering problem in sliding mode control systems. In *2006 International Workshop on Variable Structure Systems* (pp. 346–350). IEEE. https://doi.org/10.1109/VSS.2006.1644542

Utkin, V., Poznyak, A., Orlov, Y. V., & Polyakov, A. (2020). *Road map for sliding mode control design*. Springer. https://doi.org/10.1007/978-3-030-41709-3

Wang, A., Feng, X., Liu, H., & Yao, M. (2024). Design of sliding mode controller for servo feed system based on generalized extended state observer with reinforcement learning. *Scientific Reports, 14*, Article 24976. https://doi.org/10.1038/s41598-024-75598-5

Wang, N., & Adeli, H. (2012). Algorithms for chattering reduction in system control. *Journal of the Franklin Institute, 349*(8), 2687–2703. https://doi.org/10.1016/j.jfranklin.2012.06.001

Wang, Z., & Fei, J. (2022). Fractional-order terminal sliding-mode control using self-evolving recurrent Chebyshev fuzzy neural network for MEMS gyroscope. *IEEE Transactions on Fuzzy Systems, 30*(7), 2747–2758. https://doi.org/10.1109/TFUZZ.2021.3094717

Wong, C.-C., Huang, B.-C., & Lai, H.-R. (2001). Genetic-based sliding mode fuzzy controller design. *Tamkang Journal of Science and Engineering, 4*(3), 165–172. https://doi.org/10.6180/jase.2001.4.3.03

Yang, J., Shang, C., Li, Y., Li, F., & Shen, Q. (2021). ANFIS construction with sparse data via group rule interpolation. *IEEE Transactions on Cybernetics, 51*(5), 2773–2786. https://doi.org/10.1109/TCYB.2019.2952267

Yareshe, F. T., Madebo, N. W., Abdissa, C. M., & Lemma, L. N. (2025). Trajectory tracking of fixed-wing UAV using ANFIS-based sliding mode controller. *IEEE Access, 13*, 61986–62003. https://doi.org/10.1109/ACCESS.2025.3557472

Yonezawa, H., Yonezawa, A., & Kajiwara, I. (2025). Experimental verification of model-free active damping system based on virtual controlled object and fuzzy sliding mode control. *Mechanical Systems and Signal Processing, 224*, Article 111961. https://doi.org/10.1016/j.ymssp.2024.111961

Yu, X., & Efe, M. Ö. (Eds.). (2015). *Recent advances in sliding modes: From control to intelligent mechatronics*. Springer. https://doi.org/10.1007/978-3-319-18290-2

Acknowledgments: Omar Samperio Vázquez, CVU 551623. I would like to express my gratitude to the Autonomous University of the State of Hidalgo for the opportunity to pursue a Doctorate in Automation and Control, and to SECIHTI for the scholarship they awarded me for this program.

Data Availability Statement: The Dataset will be available on reasonable request.

Conflicts of Interest: The authors declare that they have no known competing financial interests or personal relationships that could have appeared to influence the work reported in this paper.